

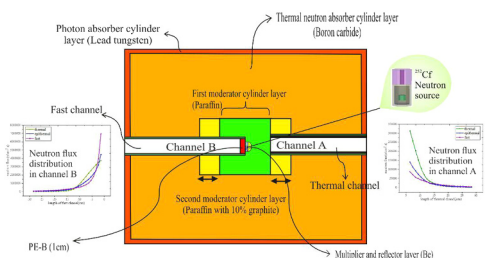
Compact shielding and irradiator design of a ^{252}Cf neutron source

Maryam Nasrabadi, Ehsan Ebrahimbababi*, Hossein Tavakoli-Anbaran

Faculty of Physics and Nuclear Engineering, Shahrood University of Technology, Shahrood, Iran



GRAPHICAL ABSTRACT



ARTICLE INFO

Keywords:
Neutron source
Moderator
Reflector
Multiplier
Absorber
MCNPX code

ABSTRACT

New developments are under way to reduce the weight and volume of neutron shielding structures using multi-layered materials. The present study aimed at designing and simulating an appropriate neutron shielding material based on a ^{252}Cf source using MCNPX code. The proposed design is composed of concentric cylinders and sphere layers with a source. The shielding matter consists of paraffin and paraffin + 10% graphite as a moderator, beryllium as a reflector and multiplier and boron carbide and lead tungsten as a thermal neutron and gamma absorber, respectively. The results indicate that, compared to previously reported shielding assemblies, the volume and the weight of the proposed design could be significantly reduced by about 97% and 75%, respectively. Thermal and fast neutron fluxes in the irradiation channel were optimized to achieve maximum values for NAA, PGNAA and other applications.

1. Introduction

Neutron sources are most useful in nuclear applications. Nuclear reactors, accelerator-based neutron sources and radioisotopes are basic neutron sources having different energy, flux and spectrum characteristics. Among these sources, radioisotope neutron sources are small, easy to handle, have a relatively low cost and do not require a high voltage source. These include spontaneous fission sources (^{252}Cf) and sources based on (α, n), (γ, n) and have applications in practical fields such as neutron activation analysis (NAA), neutron radiography, neutron capture therapy and instrument calibration (Asamoah et al., 2011; Trainer, 2002). However, they are subject to radiation protection requirements according to established standards.

Recent results show that compact shielding for radioisotope neutron sources is achievable by choosing appropriate materials for the various layers of the shield array considering appropriate neutron moderating and absorbing materials (Nasrabadi, Baghban, 2013). The present study aimed at designing a multi-layered shield for protection against a cylindrical ^{252}Cf neutron source, considering the most efficient conditions in terms of volume, weight, stability and ease of handling. In addition, this study describes the modeling of a ^{252}Cf neutron irradiator that can be used in NAA, prompt gamma neutron activation analysis (PGNAA) and other applications. All designs and simulations are based on the Monte Carlo n-particle transport (MCNPX) code.

* Corresponding author.

E-mail addresses: e.ebrahimi@shahroodut.ac.ir, ehsan.eb.64@gmail.com (E. Ebrahimbababi).

Table 1
Chemical composition and density of materials.

Composition	Materials	Density (g/cm ³)
C ₂₅ H ₅₂ , Graphite	Paraffin, 10%C	0.97
C ₂ H ₄ , Bi	PE, 5%Bi	0.98
PbWO ₄	Lead tungstate	8.24
C ₃ H ₆ , C ₂ H ₄	PE, Propylene	0.92
C ₂ H ₃ Cl	Polyvinyl Chloride	1.406
MgB ₂	Magnesium di boron	2.57
B ₄ C	Boron carbide	2.5
C ₂ H ₄ , borated	Borated PE	1
C ₂ H ₄ , Li	PE, 10%Li	0.865
Steel boron stainless	Steel, Boron Stainless	7.87
C ₂₅ H ₅₂	Paraffin	0.93
W	Tungsten	19.3
C ₅ O ₂ H ₈	Polymethyl methacrylate	1.19
ZrH ₂	Zirconium Hydride	5.61

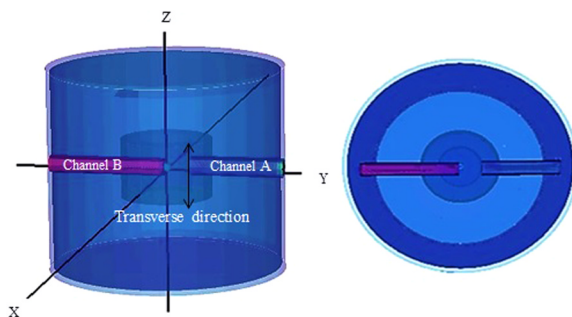


Fig. 1. 3D view of shield configuration.

2. Materials and methods

The ²⁵²Cf used had a half-life 2.645 years and decays by α -emission (96.91% probability) and spontaneous fission (3.09% probability). Because the source was encapsulated inside a pressed aluminum pellet, the alpha particles could not escape and only neutrons were considered (Martin et al., 2000; Manojlović et al., 2015). Neutron emission by the source was followed by gamma ray emissions. Gamma rays can be emitted by either spontaneous fission and fission product decay (direct gamma rays) or indirectly by gamma rays from (n, gamma) reactions (Anderson et al., 2016). The ²⁵²Cf used in this investigation was a 50 µg cylindrical source of 1 GBq activity composed of a cylinder 7.5 mm in diameter by 14 mm in length made of stainless steel. The emission rate of the neutron and gamma ray of sources was 1.15×10^8 n/s and 6.5×10^8 γ /s, respectively (Manojlović et al., 2015). The

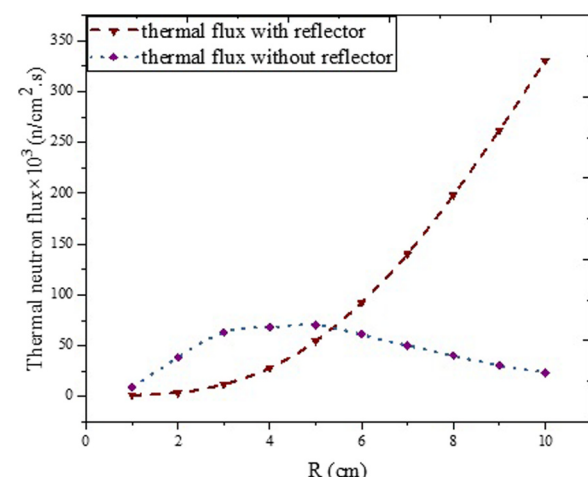


Fig. 2. Comparison of thermal neutron flux: (a) with reflector; (b) without reflector.

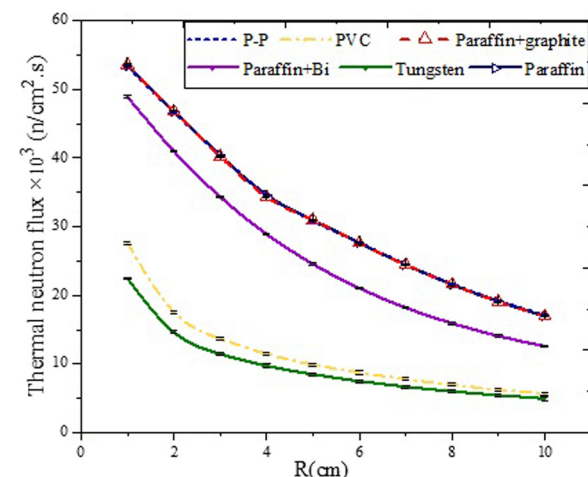


Fig. 3. Thermal neutron flux variation vs. thickness of materials in second layer.

neutron source shielding design use a low atomic number material to moderate the neutrons and high atomic number elements to absorb gamma rays (Chilton et al., 1984; Soufanidis, 1995).

Shielding effectiveness depends on parameters such as the shape, size, thickness and material used. The proposed shield configuration consisted of moderator, reflector, multiplier and absorber material in

Table 2
Maximum thermal, epithermal and fast neutrons flux vs. thickness of material.

Moderator	Top and bottom thickness(cm)	Lateral thickness(cm)	Neutron flux ^a
Paraffin	5	5	Thermal: 7.030×10^4 Epithermal: 1.002×10^5 Fast: 9.455×10^4
Polymethyl methacrylate ^b	4	4	Thermal: 4.164×10^4 Epithermal: 1.706×10^5 Fast: 1.928×10^5
Zirconium hydride ^c	4	4	Thermal: 6.969×10^4 Epithermal: 1.715×10^5 Fast: 1.622×10^5

^a n cm⁻² s⁻¹.

^b C₅O₂H₈.

^c ZrH₂.

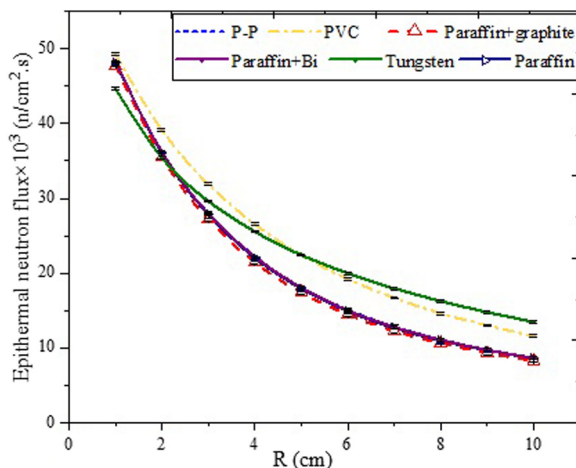


Fig. 4. Epithermal neutron flux variation vs. thickness of materials in second layer.

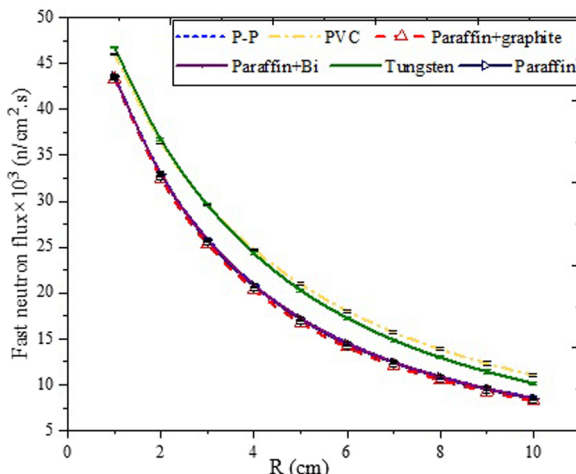


Fig. 5. Fast neutron flux vs. thickness of materials in second layer.

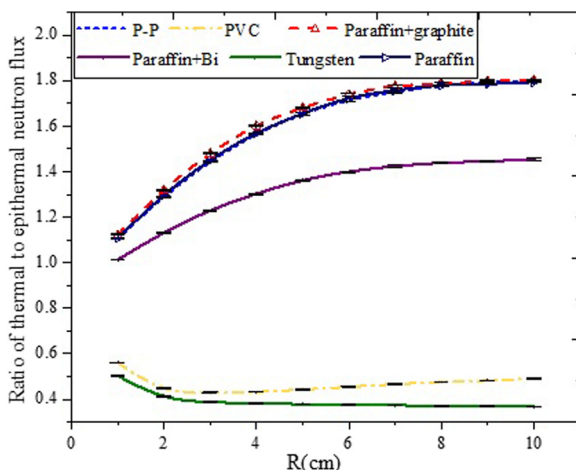


Fig. 6. Ratio of thermal neutron flux to epithermal neutron flux for materials in second layer.

layers with cylindrical and spherical geometries. The chemical composition and density of materials used in the simulations are listed in Table 1. To evaluate and optimize the neutron shielding, several Monte Carlo calculations were carried out using MCNPX code. The ranges of energy considered in the simulation were thermal neutrons (0–0.5 eV), epithermal neutrons (0.5 eV to 0.5 MeV) and fast neutrons (0.5–11 MeV). Tally F2 was used to calculate the neutron flux and the dose rate from the neutrons and gammas using flux to dose the conversion factors in ICRP (Battat, 1977; Grande, O’ Riordan chairmen, 1971). The relative error of computation was less than 0.5% for all simulations. The proposed configuration is shown in Fig. 1.

3. Results

3.1. Shielding design

The design goal for the first layer was to have high thermal neutron flux with low epithermal and fast neutron fluxes. In this layer, the material should have relatively high elastic scattering cross-sections for fast neutrons. Paraffin, polymethyl methacrylate and zirconium hydride were investigated as moderators in the layer. The maximum thermal, epithermal and fast neutron fluxes for the different thicknesses of the materials used are shown in Table 2. Based on the above-mentioned explanations and results in Table 2, paraffin was considered as the first layer material.

It should be mentioned that the epithermal and fast neutron fluxes at the beginning of the configuration were greater than the thermal neutron flux. Thus, by applying another layer as the reflector, the thermal neutron flux could be increased. Beryllium was selected as the optimal reflector because it has a low energy threshold (1.7 MeV), a large cross-section for the (n, 2n) reaction and is considered to be a neutron multiplier (Meadows et al., 1994). Based on the simulations, a 1-cm thickness for beryllium, which was a concentric spherical layer with a neutron source, was selected as the reflector before the 5-cm thickness moderator. Fig. 2 shows the thermal neutron flux distribution for configurations with and without a reflector.

The second and third layers of the shielding structures were determined using the proposed materials shown in Table 1. The ideal material for these layers was selected based on parameters such as thermal neutron flux distribution, non-thermal neutron flux distribution and ratio of thermal to non-thermal neutron flux. These parameters for paraffin + 10% graphite, polyethylene (PE), polyvinyl chloride (PVC), PE + 5% bismuth (Bi), PE + propylene (P-P) and tungsten (W) were simulated as shown in Figs. 3–7, respectively.

As shown in Figs. 3–5, thermal and non-thermal neutron flux magnitude decreased as the moderator thickness increased. The maximum thermal neutron flux magnitude in the three materials (paraffin + 10% graphite, P-P, paraffin) was very similar. The values (5-cm thickness) for paraffin + 10% graphite were 1.009 and 1.005 times higher than for the P-P and paraffin, respectively, with a relative error of 0.13%. Figs. 6 and 7 shows that the ratio of thermal neutron flux to non-thermal neutron flux increased from 1 to 5 cm and then remained nearly constant. These values for paraffin + 10% graphite were 1.046 and 1.036 times higher than for P-P and paraffin, respectively. Thus, paraffin + 10% graphite with a 5-cm thickness was selected as the second layer.

In the third layer, 1–17 cm each of borated PE, stainless steel boron, boron carbide, lead tungsten, PE + Li and magnesium di-boron were simulated as neutron and gamma absorbing materials. The neutron and gamma dose rates as a function of thickness of the materials are shown in Figs. 8 and 9, respectively. The figures indicate that boron carbide

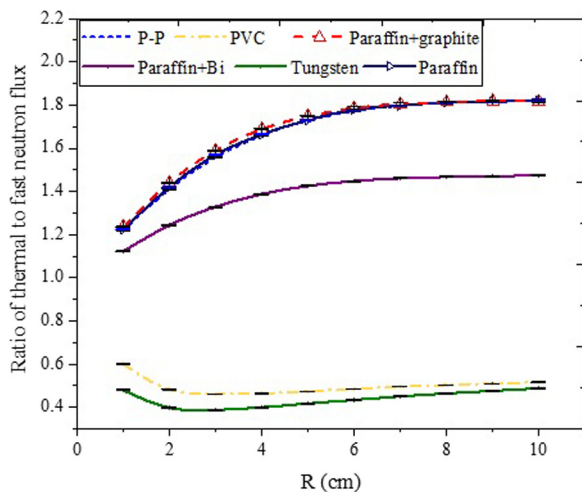


Fig. 7. Ratio of thermal neutron flux to fast neutron flux for various materials.

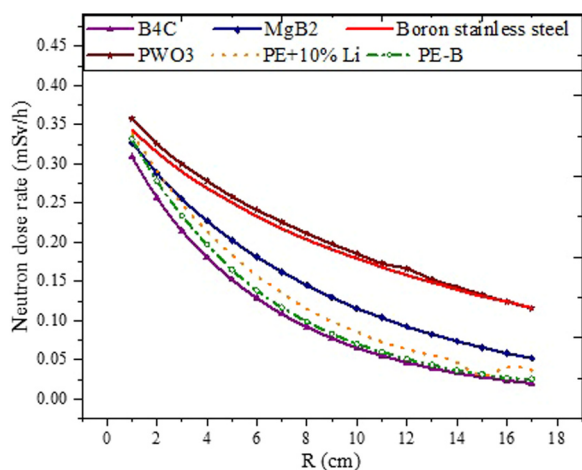


Fig. 8. Neutron dose rate for materials in third layer.

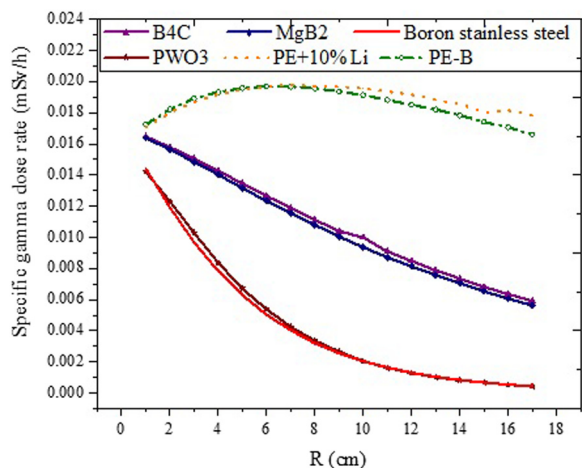


Fig. 9. Gamma dose rate for materials in third layer.

and lead tungsten had minimum levels of neutron and gamma dose rates, respectively. Boron carbide was selected as the neutron absorber material because of its large absorbing cross-section for thermal neutrons. Lead tungsten was selected as the gamma absorber because of its strong attenuating ability for gamma rays.

To obtain minimum-weight structures, this study considered various structures for the gamma and neutron absorbers in the last layer. Fig. 10(a) shows the third layer using different combinations of boron carbide and lead tungsten. The results show that the optimal structure consisted of 17 cm of boron carbide and 1 cm of lead tungsten (configuration 4).

Fig. 10(b) shows that the total gamma dose rates (direct and indirect) were lower than the neutron dose rate. The simulations show that the evaluation of dose rate at a distance of 1 m from the proposed shield was less than 0.025 mSv/h and is in accordance with ICRP recommendations (Grande, O'Riordan chairmen, 1971). In addition, mesh tallies were used to measure the neutron and gamma flux mapping inside the shield as shown in Fig. 11.

Vega-Carrillo et al. designed a water-extended polyester shield for a ²⁵²Cf neutron source. The volume and weight of their proposed design were calculated to be 1.54 m³ and 1694 kg, respectively. Based on the results shown in Table 3, the volume and weight of the proposed design with respect to traditional designs (Vega-Carrillo et al., 2007) decreased by about 97% and 75%, respectively.

3.2. Irradiator design

In the configuration, two neutron irradiators were considered for neutron activation analysis using thermal and fast neutrons. Fig. 1 shows irradiation channels A (thermal) and B (fast). Irradiation channel A consists of a horizontal cylinder filled with 0.5 cm paraffin to obtain high thermal neutron flux and 0.5 cm Fe to attenuate the gamma radiation. It is located immediately after the second layer of the shield. The length, diameter and thickness of the thermal neutron irradiator are 23 cm, 40 mm and 10 mm, respectively. Irradiation channel B is a horizontal cylinder filled with 0.25 cm bismuth and 1 cm borated PE and is located immediately after the neutron source. The length, diameter and thickness of the fast neutron irradiator are 28 cm, 40 mm and 2.5 mm, respectively. The radial neutron flux distribution from the bottom to the top of the thermal neutron channel was simulated. Fig. 12 shows the simulations of the neutron flux distributions at the end of the second layer of the shield and at the beginning of channel A.

3.3. Axial neutron flux distribution in channels A and B

In the following, tally F4 and a tally segment card (FS) were used to determine the axial change of the neutron flux distribution in irradiation channels A and B. Figs. 13 and 14 show the spectrum of the thermal, epithermal and fast neutron fluxes along irradiation channels A and channel B, respectively. The results indicate that the ratios of thermal neutron flux to epithermal neutron flux and fast neutron flux in channel A were 2.22 and 3.6, respectively. In the channel B, the ratios of fast neutron flux to thermal neutron flux and epithermal neutron flux were 1.86 and 1.55, respectively.

4. Conclusions

The effects and degree of penetration of radioactive rays differ from the shielding perspective. Although the penetration depth of charged particles through matter is very small, indirect ionizing radiation by neutrons, gamma rays and x-rays would require more shielding

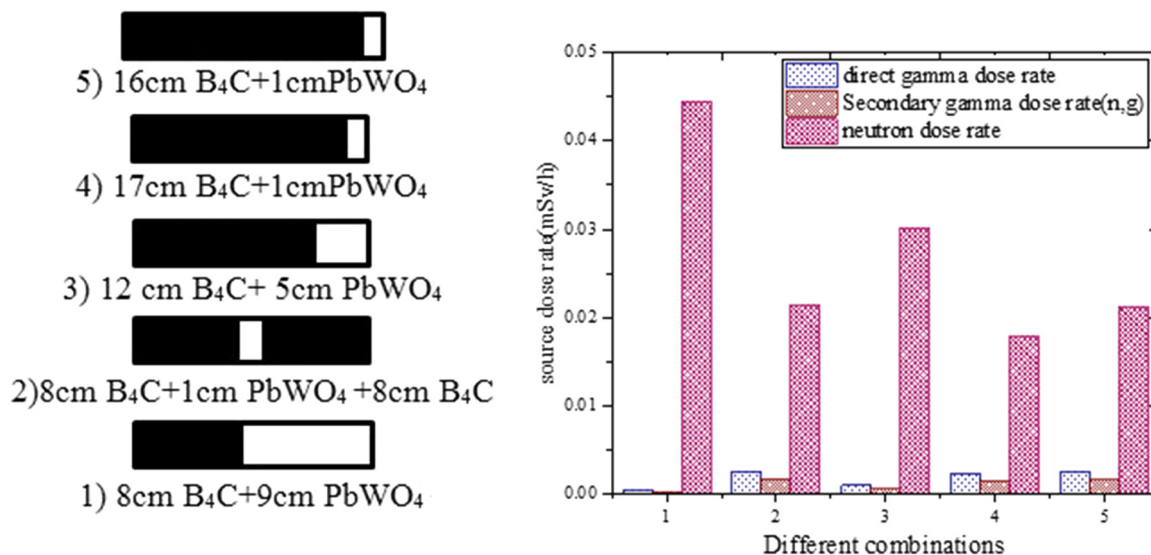


Fig. 10. (a) Different combinations of absorber layer; (b) neutron and gamma dose rates.

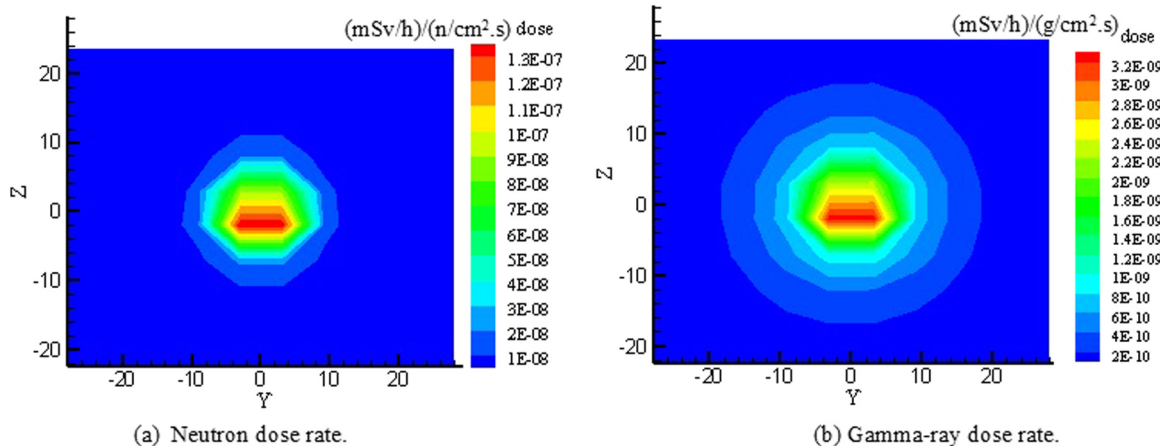
Fig. 11. Map of neutron and gamma-ray dose rates for proposed shield design for ²⁵²Cf.

Table 3
Parameters of new and conventional designs.

Parameter	Moderator	Neutron absorber	Gamma absorber	Volume(m ³)	Weight(kg)	Dose equivalent rate (mSv/h)
Old design[12]	WEP ¹	—	—	1.54	1694	0.0044
New design (our work)	Paraffin, Paraffin with10% graphite	B ₄ C ²	Lead tungsten	0.0401	417	0.0219

¹ Water-extended polyester.² Boron carbide.

material. The size and weight of the shield can be reduced by considering a multi-layered shield structure. The current study aimed to design a compact shield for a ²⁵²Cf neutron source. Different types of moderators, reflectors and absorbers were investigated and the optimal thickness for the proposed materials was determined.

The final configuration contains three-layers, 1 cm of beryllium as the reflector and multiplier and 5 cm of paraffin as the moderator in the

first layer and 5 cm paraffin + 10% graphite as the moderator in the second layer. Boron carbide and lead tungsten were selected as the neutron and gamma absorbers in the final layer of the shield as shown in Fig. 10(a). The results show that the dose rate at 1 m from the proposed shield was 0.0219 mSv/h. In addition, thermal and fast neutron radiation channels were described for use in applications such as NAA and PGNAA.

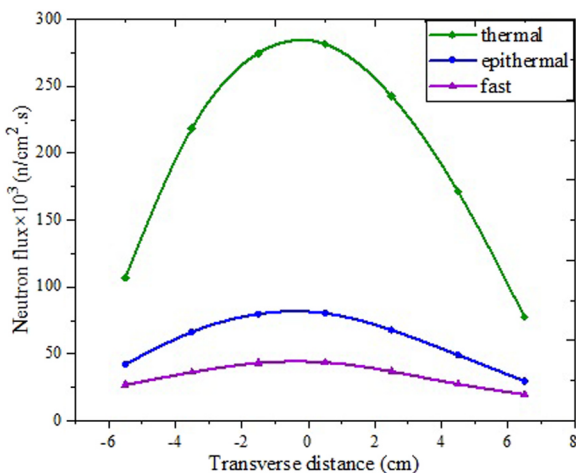


Fig. 12. Neutron flux distributions at different points along second layer.

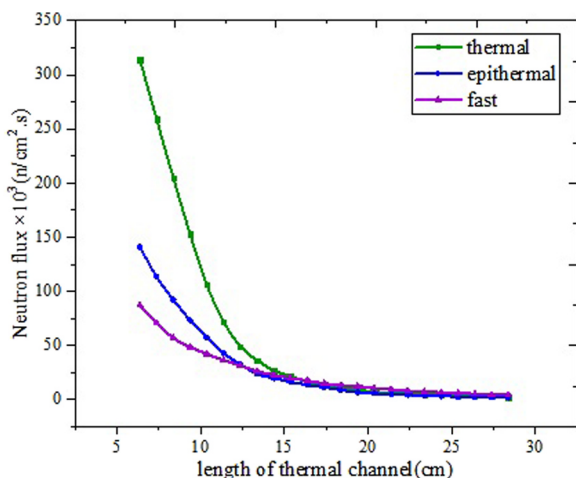


Fig. 13. Neutron flux distribution in thermal channel.

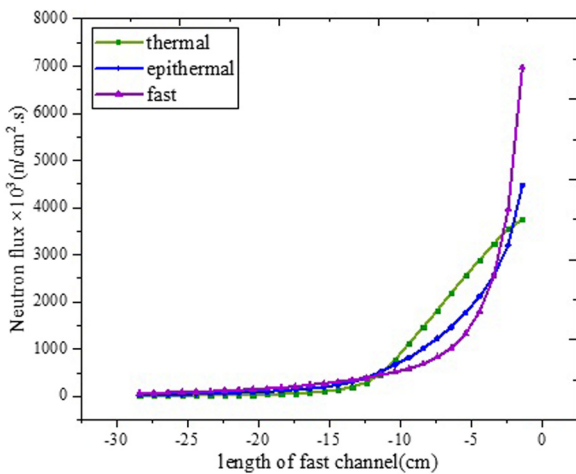


Fig. 14. Neutron flux distribution in fast channel.

References

- Anderson, B.C., Holbert, K.E., Bowler, H., 2016. Design, construction, and modeling of a ^{252}Cf neutron irradiator. *Sci. Technol. Nucl. Install.* pages.12. <https://doi.org/10.1155/2016/9012747>.
- Asamoah, M., Nyarko, B.J.B., Fletcher, J.J., Sogbadji, R.B.M., Yamoah, S., Agbemava, S.E., Mensimah, E., 2011. Neutron flux distribution in the irradiation channels of Am–Be neutron source irradiation facility. *Ann. Nucl. Energy* 38, 1219–1224. <https://doi.org/10.1016/j.anucene.2011.02.014>.
- Battat, M.E., 1977. American National Standard Neutron and Gamma-Ray Flux-to-Dose Rate Factors. ANSI/ANS-6.1.1 (N666). American Nuclear Society, LaGrange Park, Illinois (ANS – 6.1.1 Working Group).
- Chilton, A.B., Shultis, J.K., Faw, R.E., 1984. Principles of Radiation Shielding 488 Prentice Hall, Englewood Cliffs.
- Grande, P., O’Riordan chairmen, M.C., 1971. Data for Protection against Ionizing Radiation from External Sources: Supplement to ICRP Publication 15, ICRP-21. International Commission on Radiological Protection, Committee 3, Pergamon press.
- Manojlović, S., Trkov, A., Žerovnik, G., Snoj, L., 2015. Capture cross section measurement analysis in the Californium-252 spectrum with the Monte Carlo method. *Appl. Radiat. Isot.* 101–106. <https://doi.org/10.1016/j.apradiso.2015.03.023>.
- Martin, R.C., Knauer, J.B., Balo, P.A., 2000. Production, distribution and applications of californium-252 neutron sources. *Appl. Radiat. Isot.* 53, 785–792. [https://doi.org/10.1016/S0969-8043\(00\)00214-1](https://doi.org/10.1016/S0969-8043(00)00214-1).
- Meadows, J.W., Smith, D.L., Greenwood, L.R., Kneff, D.W., Oliver, B.M., 1994. Measurement of the $^9\text{Be}(\text{n},2\text{n})^8\text{Be}$ reaction cross section in the $^9\text{Be}(\text{d},\text{n})$ thick-target neutron spectrum. *Annu. Nucl. Energy* 21, 155–164. [https://doi.org/10.1016/0306-4549\(94\)90057-4](https://doi.org/10.1016/0306-4549(94)90057-4).
- Nasrabadi, M.N., Baghban, G., 2013. Neutron shielding design for ^{241}Am –Be neutron source considering different sites to achieve maximum thermal and fast neutron flux using MCNPX code. *Ann. Nucl. Energy* 59, 47–52. <https://doi.org/10.1016/j.anucene.2013.03.030>.
- Soufanidis, N.T., 1995. Measurement and Detection of Radiation. second edition. Washington; DC 200053521.
- Trainer, M., 2002. Neutron activation: an invaluable technique for teaching applied radiation. *Eur. J. Phys.* 23, 55–60. <https://doi.org/10.1088/0143-0807/23/1/308>.
- Vega-Carrillo, H.R., Manzanares-Acuña, E., Hernández-Dávila, V.M., 2007. Water-ex tended polyester neutron shield for a ^{252}Cf neutron source. *Radiat. Prot. Dosim.* 126, 269–273. <https://doi.org/10.1093/rpd/ncm056>.